

Article

Effect of Humid Aging on the Oxygen Adsorption in SnO₂ Gas Sensors

Koichi Suematsu ^{1,*} , Nan Ma ^{2,†}, Ken Watanabe ¹, Masayoshi Yuasa ^{1,‡}, Tetsuya Kida ^{1,§} and Kengo Shimanoe ¹

¹ Department of Advanced Materials Science and Engineering, Faculty of Engineering Sciences, Kyushu University, Kasuga, Fukuoka 816-8580, Japan; watanabe.ken.331@m.kyushu-u.ac.jp (K.W.); yuasa@fuk.kindai.ac.jp (M.Y.); tetsuya@kumamoto-u.ac.jp (T.K.); shimanoe.kengo.695@m.kyushu-u.ac.jp (K.S.)

² Department of Molecular and Material Science, Interdisciplinary Graduate School of Engineering Science, Kyushu University, Kasuga, Fukuoka 816-8580, Japan; manan.0611@gmail.com

* Correspondence: suematsu.koichi.682@m.kyushu-u.ac.jp; Tel.: +81-92-583-7539

† Present address: Beijing Institute of Nanoenergy and Nanosystems, Chinese Academy of Science, Beijing 100083, China.

‡ Present address: Department of Biological and Environmental Chemistry, School of Humanity-Oriented Science and Engineering, Kinki University, Iizuka, Fukuoka 820-8555, Japan.

§ Present address: Department of Applied Chemistry and Biochemistry, Kumamoto University, Kumamoto 860-8555, Japan

Received: 18 December 2017; Accepted: 11 January 2018; Published: 16 January 2018

Abstract: To investigate the effect of aging at 580 °C in wet air (humid aging) on the oxygen adsorption on the surface of SnO₂ particles, the electric properties and the sensor response to hydrogen in dry and humid atmospheres for SnO₂ resistive-type gas sensors were evaluated. The electric resistance in dry and wet atmospheres at 350 °C was strongly increased by humid aging. From the results of oxygen partial pressure dependence of the electric resistance, the oxygen adsorption equilibrium constants (K_1 ; for O[−] adsorption, K_2 ; for O^{2−} adsorption) were estimated on the basis of the theoretical model of oxygen adsorption. The K_1 and K_2 in dry and wet atmospheres at 350 °C were increased by humid aging at 580 °C, indicating an increase in the adsorption amount of both O[−] and O^{2−}. These results suggest that hydroxyl poisoning on the oxygen adsorption is suppressed by humid aging. The sensor response to hydrogen in dry and wet atmosphere at 350 °C was clearly improved by humid aging. Such an improvement of the sensor response seems to be caused by increasing the oxygen adsorption amount. Thus, the humid aging offers an effective way to improve the sensor response of SnO₂ resistive-type gas sensors in dry and wet atmospheres.

Keywords: SnO₂; gas sensors; humid aging; oxygen adsorption; hydroxyl poisoning; hydrogen sensing

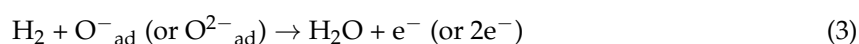
1. Introduction

Resistive-type semiconductor gas sensors using SnO₂ have been well investigated and successfully applied to commercial gas alarm systems, air quality sensors, odor sensors, and alcohol monitors for human breath since their invention 65 years ago [1–4]. SnO₂ gas sensors detect combustible gases such as hydrogen, carbon monoxide, and ethanol by a change in the electrical resistance. The electrical resistance change is derived from the interaction of adsorbed oxygen with combustible gases at approximately 250–350 °C. The gas detection mechanism of SnO₂ gas sensors is based on the reaction of adsorbed oxygen with combustible gases on the surface [5–11]. The dissociative adsorption of oxygen occurs, trapping one or two electrons from SnO₂, as expressed by the following equations:





Here, e^- is the carrier electron in SnO_2 , and O^-_{ad} and $\text{O}^{2-}_{\text{ad}}$ are the adsorbed oxygen that trapped (captured) electrons. The occurrence of such oxygen adsorption was experimentally elucidated by temperature programmed desorption (TPD)-, [8] electrical resistance-, [9] and electron spin resonance (ESR)-measurements [12]. It has been well accepted that an electron depletion region is formed on the particle surface by oxygen adsorption on cation sites (Sn^{4+}), [13] thereby increasing the electrical resistance [14,15]. When combustible gases are present in the gas phase, adsorbed oxygen disappears from the surface by a combustion reaction with gases and trapped electrons are transferred back to SnO_2 , as expressed by the following equation:



Consequently, the electrical resistance of SnO_2 decreased because of the reduction in the electron depletion region. Such a change in the electrical resistance is utilized as a signal for combustible gas detection.

Water vapor, which is always present in the atmosphere, has been recognized as the most harmful gas for semiconductor-type sensors because the adsorbed water blocks the oxygen adsorption on the surface (hydroxyl poisoning) [6,7,16–18]. The formation of hydroxyl groups on Sn^{4+} sites can be expressed by the following equation [16]:



As mentioned above, oxygen adsorption is the key process in detecting combustible gases. Thus, surface treatment of the SnO_2 surface is sometimes carried out to accelerate the oxygen adsorption. The surface treatment at high temperature (aging) is one way to eliminate adsorbed impurities such as by-products, water vapor, and carbonates on the particle surface. Such an aging process is important to understand the behavior of gas adsorption and reactions on the SnO_2 surface [19–21]. In addition, the thermal aging is often carried out for commercial sensors to stabilize the sensor signal. However, scientific investigation of the effect of aging at high temperature on the sensor response is limited to few reports [22–24]. For example, Nelli et al. reported the stabilization of the sensor response of a sensor device by aging at 400 °C for 20 days [22]. Itoh et al. also proposed that long time aging in humid atmosphere improves the sensor performance in a humid atmosphere [23]. They attributed this effect to the naturalization of the particle surface by humid air at high temperature. On the other hand, Thomas et al. reported that high temperature annealing at 325 °C recovered the sensor response to hydrocarbons for a SnO_2 semiconductor gas sensor even after its repeated use [24]. This finding implies that the aging process can refresh the particle surface to the original state. However, the annealing temperature should be sufficiently high to refresh the surface, because byproducts such as hydroxyls and carbonates that are produced by surface reaction usually desorb over 500 °C according to results on TPD measurements [6,7].

In this study, we investigated the effect of high temperature aging on the electrical and gas sensing properties of SnO_2 semiconductor gas sensor. It is expected that high temperature aging would purify the particle surface and change the oxygen adsorption behavior. We evaluated the oxygen adsorption properties and hydrogen sensing properties after aging in humid air at 580 °C. A correlation between the electrical resistance and oxygen partial pressure was examined using a theoretical model [25]. The particular emphasis was placed on the effect of water vapor during aging treatments on oxygen adsorption properties to find a promising way that improves the gas sensing properties under humid conditions.

2. Materials and Methods

2.1. Preparation and Characterization of SnO₂ Nanoparticles and Sensor Fabrication

SnO₂ nanoparticles were synthesized by hydrothermal synthesis, as described in a previous report [9]. Stannic acid gel (SnO₂·*n*H₂O), which is obtained by mixing a SnCl₄·5H₂O (Wako Pure Chemical Industries, Ltd., Osaka, Japan) solution (1 M) into NH₄HCO₃ (Kishida Chemical Company, Ltd., Osaka, Japan) solution (1 M), was hydrothermally treated at 200 °C for 3 h using an autoclave system (TAS-05 type; TAIATSU TECHNO, Tokyo, Japan) after Cl[−] ions were removed and the solution pH was adjusted to 10.5. Then, the obtained SnO₂ dispersed sol was dried in air at 120 °C for a half day, and then calcined at 600 °C for 3 h, producing a SnO₂ powder. A paste containing the SnO₂ powder in an organic binder (α -terpineol; Wako Pure Chemical Industries, Ltd.) was coated on an Al₂O₃ substrate (9 mm × 13 mm × 0.38 mm; Japan Fine Ceramics Company, Ltd., Miyagi, Japan) equipped with comb type Au electrodes (electrode span is 90 μ m, sensing layer area is 64 mm²) by a screen printing method to fabricate a thick film-type sensor device. Then, the device was heated at 580 °C for 3 h in air to remove α -terpineol. The schematic image and photographs of the Au electrode and sensor device are shown in Figure 1a.

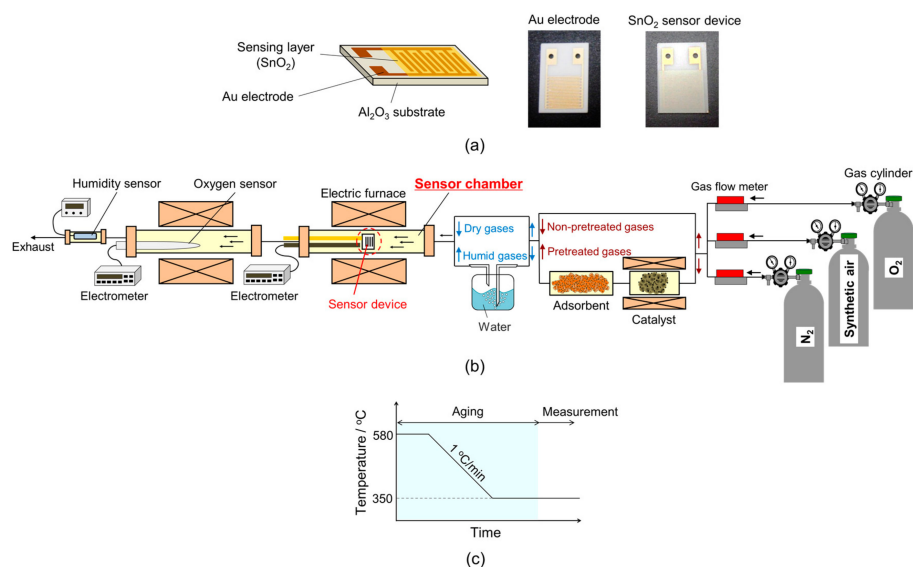


Figure 1. (a) Schematic image and photographs of the Al₂O₃ substrate printed with Au electrode and SnO₂ sensor device. (b) Schematic drawing of the measurement apparatus and sensor device for gas sensors. (c) Temperature profile of the aging process.

The crystal structure of the SnO₂ particles was determined by X-ray diffractometry with copper K α radiation (XRD; RINT 2100, RIGAKU, Tokyo, Japan), and the crystallite size was estimated from the Sherrer's equation. The specific surface area of SnO₂ particles was measured using a specific surface area analyzer (BELSORP-mini II; Bel Japan, Osaka, Japan). The obtained nanoparticles were observed by field-emission scanning electron microscopy (FE-SEM; S-4800, Hitachi, Tokyo, Japan).

2.2. Evaluation of the Electrical Properties

The electrical resistance was measured with an apparatus equipped with a gas pretreatment system, a water vapor introduction system, an oxygen sensor, and a humidity sensor, as schematically described in Figure 1b. The gas pretreatment system was equipped with a catalyst and an adsorbent of Pt (5 wt %)-loaded Al₂O₃ (Wako Pure Chemical Industries, Ltd.) and molecular sieves (5A 1/16, Wako Pure Chemical Industries Ltd.), respectively [9,26]. The catalyst was heated at 500 °C to remove impurities from commercial nitrogen and air. Water vapor was introduced through a bubbler containing

de-ionized water, and the humidity was controlled by mixing dry and humid gases. The exact P_{O_2} and humidity (partial pressure of H_2O ; P_{H_2O}) in the gas atmosphere were measured with a homemade oxygen sensor based on calcium stabilized zirconia (CSZ; Suzuki rikagaku Co., Ltd., Okegawa, Japan) and a commercial capacitance-type humidity sensor (TR-77Ui; T&D Corporation, Matsumoto, Japan), respectively. Temperature around the sensor device was monitored by a thermocouple that was positioned close to the sensor device. The gas flow rates of air and sample gases were adjusted to $80 \text{ cm}^3/\text{min}$ with mass flow controllers (SEC-series; HORIBA STEC, Kyoto, Japan).

The temperature profile of thermal aging of devices is shown in Figure 1c. Thermal aging was carried out at $580 \text{ }^\circ\text{C}$ for 3 h in air with different humidity levels. Then, the device was cooled down to $350 \text{ }^\circ\text{C}$ and the electrical resistance was measured after the resistance had stabilized. For the measurements, P_{O_2} was adjusted by mixing nitrogen, synthetic air or oxygen. These gases were purified with the gas pretreatment system. Sample gases containing hydrogen in air were prepared by diluting parent synthetic gas mixture with purified synthetic air. In this case, parent synthetic gas mixtures containing hydrogen were not treated with the gas pretreatment system. The sensor device was connected with a standard resistor, and voltage across the standard resistor was measured under an applied voltage of DC 4 V to evaluate the electrical resistance of the device. The electrical signal of the sensor was acquired with an electrometer (Model 12002; Keithley Instruments, Cleveland, OH, USA), and the relative resistance and sensor response to hydrogen were defined as R/R_{N_2} and R_a/R_g , respectively. Here, R , R_{N_2} , R_a and R_g are the electrical resistance in various P_{O_2} , nitrogen, synthetic air and sample gases, respectively.

3. Results and Discussion

3.1. Effect of Humid Aging on the Material Characteristics

Figure 2a shows the XRD patterns of SnO_2 nanoparticles calcined at $600 \text{ }^\circ\text{C}$ in air with and without aging in humidified oxygen (P_{H_2O} : 0.04 atm (96 RH% at $30 \text{ }^\circ\text{C}$)) at $580 \text{ }^\circ\text{C}$ for 3 h (humid aging). These XRD patterns were well matched with those of cassiterite stannic acid (JCPDS 41-1445). No impurity phases were observed. The estimated crystallite sizes of SnO_2 nanoparticles without and with humid aging were 12 and 14 nm, respectively. The SnO_2 nanoparticles slightly grew up after the humid aging. However, no further crystal growth was not observed even after repeated humid aging. Specific surface areas of the SnO_2 nanoparticles without and with the humid aging were 27 and $24 \text{ m}^2 \cdot \text{g}^{-1}$, respectively. No significant change in the surface area was observed after the humid aging. The SEM images of the SnO_2 nanoparticles confirmed no obvious difference in morphology after the humid aging, as shown in Figure 2b. The above results conclude that the humid aging slightly facilitated the growth of SnO_2 crystals, consequently reducing their specific surface area.

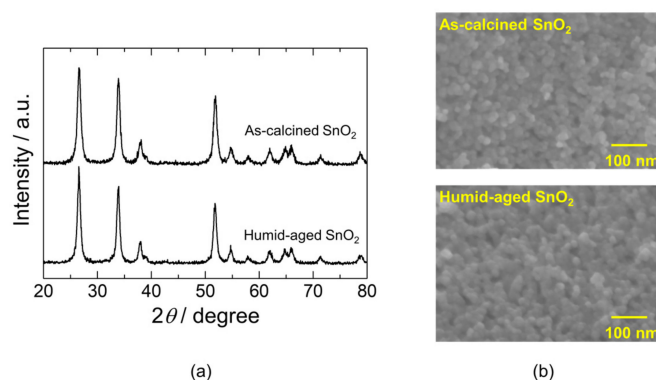


Figure 2. (a) XRD patterns and (b) SEM images of as-calcined and humid-aged SnO_2 nanoparticles.

3.2. Effect of Humid Aging on the Oxygen Adsorption

Figure 3a shows the electrical resistance at 350 °C in dry air of the device that was aged at 580 °C in humid atmosphere (humid aging) as a function of humidity at the humid aging. Here, P_{O_2} at the aging process was kept at 0.21 atm (synthetic air) and P_{H_2O} at the aging process was controlled from 0.039 atm (93 RH% at 30 °C) to 0.002 atm (6.4 RH% at 25 °C). Aging was also carried out in dry air at 580 °C (dry aging). The electrical resistance at 350 °C in dry air drastically increased after introducing water vapor during the aging processes. The larger the humidity at the aging process at 580 °C, the larger the electrical resistance in air at 350 °C was, as shown in the inset of Figure 3a. Generally, the presence of the humidity decreases the electrical resistance of SnO₂ gas sensors due to the hydroxyl poisoning on the particle surface, blocking the oxygen adsorption and decreasing the resistance. [16] In contrast, the tendency observed here is opposite to that reported as the hydroxyl poisoning effect. The resistance at 350 °C increased in dry air after the humid aging. The results here clearly indicate that the humid aging at 580 °C promoted the oxygen adsorption at 350 °C. According to some previous reports, high temperature aging can remove adsorbed gases from the particle surface. For example, a TPD analysis shows that desorption of adsorbed hydroxyls occurs at temperatures higher than 300 °C [6,7]. Thus, it is possible that hydroxyl groups desorbed from the SnO₂ surface at 350 °C, assisting in the adsorption of oxygen on the surface and increasing the electrical resistance.

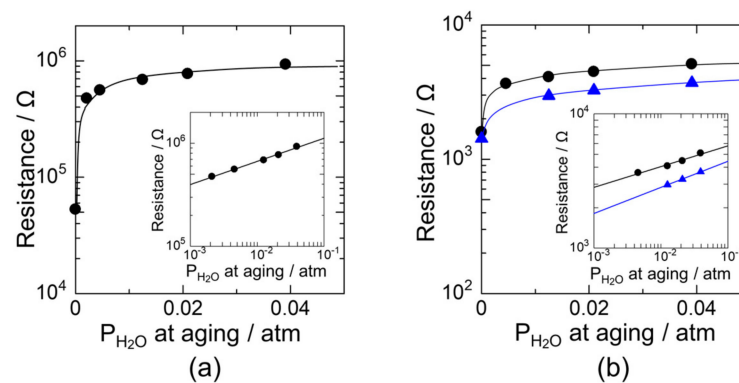


Figure 3. The electrical resistance of SnO₂ nanoparticles in (a) dry and (b) wet air atmosphere at 350 °C as a function of P_{H_2O} in humid aging. P_{H_2O} in wet air atmosphere are 0.005 and 0.01 atm.

We also measured the electrical resistance at 350 °C in wet air after the humid aging at 580 °C, as shown in Figure 3b. Here, the humidity in wet air at 350 °C was set to 0.01 atm (32 RH% at 25 °C) and 0.005 atm (16 RH% at 25 °C). The electrical resistance in wet air was much lower than that in dry air. The electrical resistance at 350 °C was 5.3×10^4 to 9.3×10^5 Ω in dry air, but it decreased to 1.6 – 5.0×10^3 Ω in wet air (P_{H_2O} : 0.005 atm) even after the humid aging, as shown in Figure 3a,b. This indicates that the hydroxyl poisoning occurred to the device. However, it is noteworthy that increasing the humidity during the humid aging increased the electrical resistance in wet air at 350 °C. This phenomenon suggests that humid aging can weaken the hydroxyl poisoning effect.

Recently, the relationship between the electrical resistance and P_{O_2} has been theoretically proposed as the following equation [25]:

$$\frac{R}{R_0} = \frac{1}{2} \left(c + \frac{3}{a} K_1^{\frac{1}{2}} P_{O_2}^{\frac{1}{2}} \right) + \left\{ \frac{1}{4} \left(c + \frac{3}{a} K_1^{\frac{1}{2}} P_{O_2}^{\frac{1}{2}} \right)^2 + \frac{6N_D}{a} \cdot K_2^{\frac{1}{2}} P_{O_2}^{\frac{1}{2}} \right\}^{\frac{1}{2}} \quad (5)$$

Here, R/R_0 is the relative resistance, R and R_0 are the electrical resistance in the atmosphere with and without oxygen, respectively, a is the crystallite radius, c is the constant value, N_D is the donor density, and P_{O_2} is the oxygen partial pressure. K_1 and K_2 are equilibrium constants, which are the

ratio of the rate constants of the forward and reverse reactions of the Equations (1) and (2), respectively. Here, if K_1 or K_2 is zero, Equation (5) can be more simplified as the following equations, respectively.

$$\frac{R}{R_0} = c + \frac{3}{a} K_1^{\frac{1}{2}} P_{O_2}^{\frac{1}{2}} \quad (O^- \text{ formation, } K_2 = 0) \quad (6)$$

$$\frac{R}{R_0} = \left\{ \frac{1}{4} c^2 + \frac{6N_D}{a} \cdot K_2^{\frac{1}{2}} P_{O_2}^{\frac{1}{2}} \right\}^{\frac{1}{2}} \quad (O^{2-} \text{ formation, } K_1 = 0) \quad (7)$$

Recently, we have evaluated the oxygen adsorption species by the linear relationship between the electrical resistance and $P_{O_2}^{1/2}$ or $P_{O_2}^{1/4}$ using the Equations (6) and (7), respectively. According to our previous report, oxygen dissociatively adsorbed as O^{2-} on the SnO_2 surface at 350 °C in dry atmosphere. The adsorption of O^{2-} is supported by the fact that the electrical resistance is proportional to the $P_{O_2}^{1/4}$ [9,27]. However, there is a possibility that the adsorption of O^- and O^{2-} occur competitively. Thus, in this study, we tried to estimate the equilibrium constants (oxygen adsorption ability) of O^- and O^{2-} adsorption using the Equation (5) by examining the correlation between the relative resistance and P_{O_2} . We expected that humid aging affects the oxygen adsorption properties, leading to a change in K_1 and K_2 values.

The relative resistance, (R/R_{N_2}), at 350 °C after the dry and humid aging was plotted as a function of P_{O_2} are shown in Figure 4a. We used the electrical resistance in N_2 (R_{N_2}) in wet atmosphere in place of the resistance without oxygen (R_0) because complete removal of oxygen from nitrogen is experimentally difficult. The nitrogen gas used in this study contained approximately 50 ppm oxygen. This residual oxygen has a strong influence on R_{N_2} . For example, R_{N_2} values in dry and wet atmospheres were 3.7×10^3 and $1.3 \times 10^2 \Omega$, respectively. Difference of these electrical resistances was caused by the oxygen adsorption amount because hydroxyl poisoning disturbs the oxygen adsorption. The lower electrical resistance in wet atmosphere indicate that the adsorption of residual oxygen in N_2 was blocked by humidity. Thus, R_{N_2} in wet atmosphere seems to be closer to the value of R_0 than R_{N_2} in dry atmosphere. Because of this reason, we used R_{N_2} in wet atmosphere in place of R_0 . Here, P_{H_2O} in the humid aging was controlled at 0.04 atm (96 RH% at 30 °C). Aging was also carried out in dry air (0 RH%, dry aging). The relative resistance clearly increased by the humid aging, as shown in Figure 4a. It should be noted that the relative resistance corresponds to the sensitivity to oxygen. Thus, the increase in the relative resistance indicates that the amount of oxygen adsorption increased after the humid aging. The results were in perfect fit with Equation (5), as shown in Figure 4a. Using the fitting results, we estimated the oxygen adsorption equilibrium constants for O^- adsorption (K_1) and O^{2-} adsorption (K_2) after the dry or humid aging. Here, the donor density of SnO_2 was set to $5.0 \times 10^{18} \text{ cm}^{-3}$, as reported in literature [15]. Dimensions of K_1 and K_2 can be derived from Equations (1) and (2), respectively, when dimensions of the surface oxygen concentration [O^-] (or [O^{2-}]) and the electron density [e^-] were cm^{-2} and cm^{-3} , respectively. The estimated K_1 and K_2 values are summarized in Table 1. Absolute K_1 and K_2 values after the humid aging are about four and five orders larger than those after the dry aging. Increases in K_1 and K_2 indicate the increase in the adsorbed oxygen amount. Thus, the obtained results conclude that the humid aging increased the amount of adsorbed oxygen as both forms of O^- and O^{2-} .

Table 1. Estimated equilibrium constants of oxygen adsorption for O^- (K_1) and O^{2-} (K_2) at 350 °C in dry air. The device was aged under dry and humid conditions.

P_{H_2O} in Aging Atmosphere/atm	Measurement Atmosphere	K_1 ($\text{cm}^2 \cdot \text{atm}^{-1}$)	K_2 ($\text{cm}^8 \cdot \text{atm}^{-1}$)
dry	dry	8×10^{-11}	8×10^{-41}
0.04 (wet)	dry	5×10^{-7}	3×10^{-36}

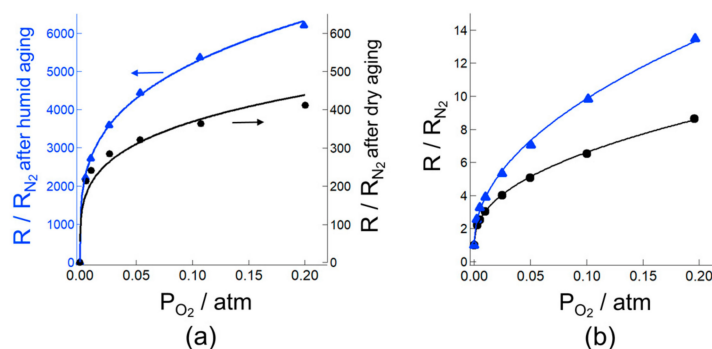


Figure 4. (a) The relative resistance (R/R_{N_2}) at 350 °C in (a) dry and (b) humid (P_{H_2O} : 0.012 atm) atmosphere as a function of oxygen partial pressure after (●) dry and (▲) humid aging.

The oxygen adsorption behaviors in wet air at 350 °C after humid aging were also studied. Figure 4b shows the relative resistance at 350 °C in wet air (P_{H_2O} : 0.012 atm, 38 RH% at 25 °C) after the dry and humid aging. Humid aging was carried out in air containing 0.05 atm H_2O (100 RH% at 33 °C). Aging was also carried out in dry air. The relative resistance in wet air increased after the humid aging. This trend is consistent with the case for the relative resistance measurements in dry air (Figure 4a). However, the absolute value of the relative resistance in wet air is significantly smaller than that in dry air, suggesting that hydroxyl poisoning occurred in wet air. Nevertheless, the results were also well fitted with Equation (5), as shown in Figure 4b. The estimated K_1 and K_2 values are summarized in Table 2. The K_1 value ($4 \times 10^{-11} \text{ cm}^2 \cdot \text{atm}^{-1}$) in wet air after humid aging is larger than that ($1 \times 10^{-11} \text{ cm}^2 \cdot \text{atm}^{-1}$) after dry aging, indicating that the amount of the O^- adsorption was increased by the humid aging. In contrast, the K_2 value in wet air after the humid aging is smaller than that after dry aging. The results suggest that hydroxyl poisoning was more significant in the O^{2-} adsorption. The significant decrease in K_2 ($7 \times 10^{-50} \text{ cm}^8 \cdot \text{atm}^{-1}$) in wet air is also prominent by comparing the values with those ($3 \times 10^{-49} \text{ cm}^8 \cdot \text{atm}^{-1}$) in dry air (Table 1), suggesting that the O^- adsorption became predominant in wet air. In the previous report, we demonstrated that the main oxygen adsorption species is transferred from O^{2-} to O^- by introducing water vapor in a measurement atmosphere [27]. Thus, the observed changes in K_1 and K_2 are in good agreement with the previous results. Recently, Watanabe et al. reported that exchanges of surface oxygen with atmospheric oxygen efficiently proceeds on indium-gallium-zinc oxide in the presence of humidity [28]. On the basis of their work, it might be possible that the oxygen adsorption on the SnO_2 surface proceeds via oxygen exchange at hydroxyl groups that were formed at high temperature during humid aging. Hence, humid aging leads to increasing the amount of oxygen adsorption on the SnO_2 than dry aging. The proposed oxygen adsorption model was schematically shown in Figure 5. The surface naturalization by humid aging, which is empirically known as an effective way to improve the sensor response in practical gas sensors, may also contribute to the increase in the amount of oxygen adsorption. However, unfortunately, no experimental evidences to support these ideas have been obtained yet. Nevertheless, we can conclude that the humid aging is one of the efficient approaches to enhance the oxygen adsorption on the SnO_2 surface even in humid atmospheres.

Table 2. Estimated equilibrium constants of oxygen adsorption for O^- (K_1) and O^{2-} (K_2) at 350 °C in wet air. The device was aged under dry and humid conditions.

P_{H_2O} in Aging Atmosphere/atm	Measurement Atmosphere	$K_1/\text{cm}^2 \cdot \text{atm}^{-1}$	$K_2/\text{cm}^8 \cdot \text{atm}^{-1}$
dry	0.012 (wet)	1×10^{-11}	3×10^{-49}
0.05 (wet)	0.012 (wet)	4×10^{-11}	7×10^{-50}

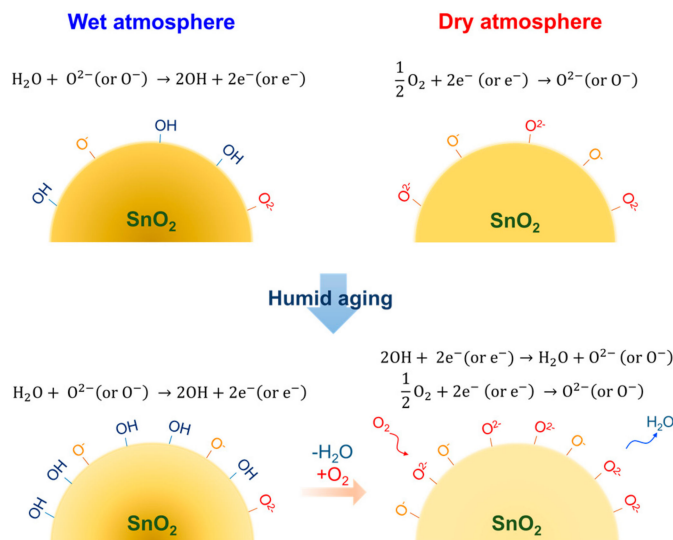


Figure 5. Schematic model of the effect of humid aging for oxygen adsorption on the SnO₂ surface in dry and wet atmospheres.

3.3. Effects of Humid Aging on the Sensor Response to Hydrogen

The sensor response to the combustible gases ($S = R_a/R_g$) is defined as the ratio of the electrical resistance in air (R_a) to that in air containing combustible gases (R_g). The electrical resistance in air is used as a base line. According to this definition, an increase in R_a should result in an increase in the sensor response. Hence, we expected that the sensor response would be enhanced by humid aging that suppresses hydroxyl poisoning of oxygen adsorption.

Figure 6 shows the sensor response to 200 ppm hydrogen in dry air at 350 °C as a function of $P_{\text{H}_2\text{O}}$ during aging for the device with humid aging at 580 °C. The sensor response was improved by the humid aging with higher humidities, as expected above. Thus, humid aging is effective in enhancing the sensor response to hydrogen because of the promotion of the oxygen adsorption.

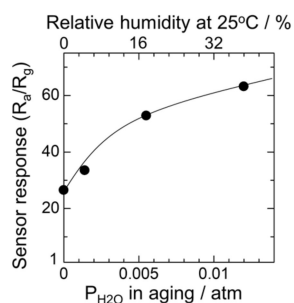


Figure 6. The sensor response to 200 ppm hydrogen at 350 °C in dry atmosphere as a function of $P_{\text{H}_2\text{O}}$ in aging.

Next, the sensor response in wet air was examined for the device with humid aging ($P_{\text{H}_2\text{O}}$: 0.03 atm, 96 RH% at 25 °C) at 580 °C. Figure 7 shows the sensor responses to hydrogen as a function of humidity in sample gases ($P_{\text{H}_2\text{O}}$: 0–0.03 atm) at 350 °C. The sensor response was significantly deteriorated by humidity for the device with the dry aging. In contrast, such a significant decrease in the sensor response was suppressed after the humid aging. As shown in Figure 4b, we observed that humid aging enhanced the oxygen adsorption. Thus, an increase in the amount of oxygen on the surface by the humid aging facilitated the combustion of hydrogen, thereby suppressing the hydroxyl poisoning [16–18]. However, in high wet air ($P_{\text{H}_2\text{O}}$: 0.03 atm), the sensor response became less than $S = 10$. Hence, further modification of the surface

conditions is necessary. Thus, the results demonstrate that humid aging is effective in improving the sensor response in wet atmospheres, especially at 350 °C.

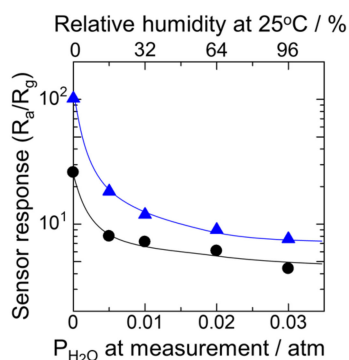


Figure 7. Relationships between the sensor response to 200 ppm H₂ at 350 °C as a function of P_{H₂O} in measurement after (●) dry and (▲) humid aging (P_{H₂O} is 0.03 atm).

4. Conclusions

In this study, we investigated the effect of aging at 580 °C in wet air (humid aging) on the oxygen adsorption and gas sensing properties for SnO₂ resistive-type gas sensors. We found that humid aging slightly increased the crystallite size, leading to a slight decrease in the specific surface area of SnO₂ nanoparticles. However, no significant difference in morphology was seen by SEM observations before and after the humid aging. In contrast, the humid aging strongly affected the electrical properties of the SnO₂ nanoparticles. The electrical resistance in air was drastically increased by the humid aging process. By analyzing the relationship between the resistance and P_{O₂}, we revealed increases of the oxygen adsorption equilibrium constants (K_1 and K_2) after humid aging. These increases in K_1 and K_2 appeared not only in a dry atmosphere but also in a humid atmosphere. Thus, hydroxyl poisoning was suppressed by humid aging that increases the amount of oxygen adsorption. Consequently, the sensor response to hydrogen was improved by the humid aging. Such an improvement in the sensor response was also confirmed even in a wet atmosphere. Therefore, we conclude that humid aging is an efficient way to enhance the oxygen adsorption on the SnO₂ surface and consequently improve the sensor response to combustible gases in dry and wet atmospheres. We also believe that this finding is important in fundamental understanding on the influence of humidity for practical gas sensors.

Acknowledgments: The authors are grateful to Miyuki Sasaki for helping them with experiment. The authors thank the Fukuoka Industrial Technology Center for observation of FE-SEM images. This work was partially supported by FIGARO Engineering Inc. This work was partially supported by JSPS KAKENHI Grant Number JP16H04219 and JP17K17941.

Author Contributions: T.K. and K.Sh. conceived and designed the experiments; K.Su. and N.M. performed the experiments; K.Su. analyzed the data; K.W. and M.Y. contributed materials and analysis tools; K.Su. wrote the paper.

Conflicts of Interest: The authors declare no conflict of interest.

References

1. Taguchi, N. Metal Oxide Gas Sensor. Japan Patent No. S45-38200, 1962.
2. Ihokura, K.; Tanaka, K.; Murakami, N. Use of tin dioxide sensor to control a domestic gas heater. *Sens. Actuat.* **1983**, *4*, 607–612. [[CrossRef](#)]
3. Homepage of Figaro Engineering Inc. Available online: <http://www.figaro.co.jp/en/> (accessed on 10 January 2018).
4. Homepage of Nissha FIS Inc. Available online: <http://www.fisinc.co.jp/en/products/> (accessed on 10 January 2018).

5. Clifford, P.K.; Tuma, D.T. Characteristics of semiconductor gas sensors I. Steady state gas response. *Sens. Actuat.* **1982/1983**, *3*, 233–254. [[CrossRef](#)]
6. Yamazoe, N.; Fuchigami, J.; Kishikawa, M.; Seiyama, T. Interactions of tin oxide surface with O₂, H₂O and H₂. *Surf. Sci.* **1979**, *86*, 335–344. [[CrossRef](#)]
7. Tamaki, J.; Nagaishi, M.; Teraoka, Y.; Miura, N.; Yamazoe, N.; Moriya, K.; Nakamura, Y. Adsorption behavior of CO and Interfering gases on SnO₂. *Surf. Sci.* **1989**, *221*, 183–196. [[CrossRef](#)]
8. Gurlo, A. Interplay between O₂ and SnO₂: Oxygen ionosorption and spectroscopic evidence for adsorbed oxygen. *ChemPhysChem* **2006**, *7*, 2041–2052. [[CrossRef](#)] [[PubMed](#)]
9. Suematsu, K.; Yuasa, M.; Kida, T.; Yamazoe, N.; Shimano, K. Determination of Oxygen Adsorption on SnO₂: Exact Analysis of Gas Sensing Properties Using a Sample Gas Pretreatment System. *J. Electrochem. Soc.* **2014**, *161*, B123–B128. [[CrossRef](#)]
10. McAleer, J.F.; Moseley, P.T.; Norris, J.O.W.; Williams, D.E. Tin dioxide gas sensors. *J. Chem. Soc. Faraday Trans. I* **1987**, *83*, 1323–1346. [[CrossRef](#)]
11. Barsan, N.; Weimar, U. Conduction Model of Metal Oxide Gas Sensors. *J. Electroceram.* **2001**, *7*, 143–167. [[CrossRef](#)]
12. Mizokawa, Y.; Nakamura, S. ESR and Electric Conductance Studies of Fine-Powdered SnO₂. *Jpn. J. Appl. Phys.* **1975**, *14*, 779–788. [[CrossRef](#)]
13. Kocemba, I.; Rynkowski, J.M. The effect of oxygen adsorption on catalytic activity of SnO₂ in CO oxidation. *Catal. Today* **2011**, *169*, 192–199. [[CrossRef](#)]
14. Ogawa, H.; Nishikawa, M.; Abe, A. Hall measurement studies and electrical conduction model of tin oxide ultrafine particle films. *J. Appl. Phys.* **1982**, *53*, 4448–4455. [[CrossRef](#)]
15. Oprea, A.; Moretton, E.; Barsan, N.; Becker, W.J.; Wöllenstein, J.; Weimar, U. Conduction model of SnO₂ thin films based on conductance and Hall effect measurement. *J. Appl. Phys.* **2006**, *100*, 033716. [[CrossRef](#)]
16. Koziej, D.; Barsan, N.; Weimar, U.; Szuber, J.; Shimano, K.; Yamazoe, N. Water-oxygen interplay on tin dioxide surface: Implication on gas sensing. *Chem. Phys. Lett.* **2005**, *410*, 321–323. [[CrossRef](#)]
17. Pavelko, R.G.; Daly, H.; Hardacre, C.; Vasiliev, A.A.; Llobet, E. Interaction of water, hydrogen and their mixtures with SnO₂ based materials: the role of surface hydroxyl groups in detection mechanisms. *Phys. Chem. Chem. Phys.* **2010**, *12*, 2639–2647. [[CrossRef](#)] [[PubMed](#)]
18. Suematsu, K.; Ma, N.; Yuasa, M.; Kida, T.; Shimano, K. Surface-modification of SnO₂ nanoparticles by incorporation of Al for the detection of combustible gases in a humid atmosphere. *RSC Adv.* **2015**, *5*, 86347–86354. [[CrossRef](#)]
19. Tanaka, K.; Morimoto, T.; Sonoda, S.; Matsuura, S.; Moriya, K.; Egashira, M. Combustion monitoring sensor using tin dioxide semiconductor. *Sens. Actuat. B* **1991**, *3*, 247–253. [[CrossRef](#)]
20. Ansari, S.G.; Ansari, Z.A.; Kadam, M.R.; Karekar, R.N.; Aiyer, R.C. The effect of humidity on an SnO₂ thick-film planar resistor. *Sens. Actuat. B* **1994**, *21*, 159–163. [[CrossRef](#)]
21. Nicoletti, S.; Dori, L.; Corticelli, F. Tin Oxide Thin-Films for Aromatic Hydrocarbons Detection: Effect of Aging Time on Film Microstructure. *J. Am. Ceram. Soc.* **1999**, *82*, 1201–1206. [[CrossRef](#)]
22. Nelli, P.; Faglia, G.; Sberveglieri, G.; Cereda, E.; Gabetta, G.; Dieguez, A.; Romano-Rodriguez, A.; Morante, J.R. The aging on SnO₂-Au thin film sensors: electrical and structural characterization. *Thin Solid Films* **2000**, *371*, 249–253. [[CrossRef](#)]
23. Ito, T.; Matsubara, I.; Kadosaki, M.; Sakai, Y.; Shin, W.; Izu, N.; Nishibori, M. Effects of High-Humidity Aging on Platinum, Palladium, and Gold Loaded Tin Oxide—Volatile Organic Compound Sensors. *Sensors* **2010**, *2010*, 6513–6521. [[CrossRef](#)] [[PubMed](#)]
24. Skariah, B.; Naduvath, J.; Thomas, B. Effect of long term ageing under humid environment on the LPG sensing properties and the surface composition of Mg-doped SnO₂ thin films. *Ceram. Int.* **2016**, *42*, 7490–7498. [[CrossRef](#)]
25. Yamazoe, N.; Suematsu, K.; Shimano, K. Extension of receptor function theory to include two types of adsorbed oxygen for oxide semiconductor gas sensors. *Sens. Actuat. B* **2012**, *163*, 128–135. [[CrossRef](#)]
26. Suematsu, K.; Yamada, K.; Yuasa, M.; Kida, T.; Shimano, K. Evaluation of Oxygen Adsorption Based on the Electric Properties of SnO₂ Semiconductor Gas Sensors. *Sens. Mater.* **2016**, *28*, 1211–1217.

27. Ma, N.; Suematsu, K.; Yuasa, M.; Kida, T.; Shimano, K. Effect of Water Vapor on Pd-Loaded SnO₂ Nanoparticles Gas Sensor. *ACS Appl. Mater. Interfaces* **2015**, *7*, 5863–5869. [[CrossRef](#)] [[PubMed](#)]
28. Watanabe, K.; Lee, D.H.; Sakaguchi, I.; Nomura, K.; Kamiya, T.; Haneda, H.; Hosono, H.; Ohashi, N. Surface reactivity and oxygen migration in amorphous indium-gallium-zinc oxide films annealed in humid atmosphere. *Appl. Phys. Lett.* **2013**, *103*, 201904. [[CrossRef](#)]



© 2018 by the authors. Licensee MDPI, Basel, Switzerland. This article is an open access article distributed under the terms and conditions of the Creative Commons Attribution (CC BY) license (<http://creativecommons.org/licenses/by/4.0/>).